Design constraints in an operon circuit for engineered control of metabolic networks

Diego A. Oyarzún[†] and Guy-Bart Stan[†]

***Abstract*— We consider a synthetic gene circuit aimed at regulating the flux through an unbranched metabolic network. The control circuit has an operon architecture whereby the expression of all pathway enzymes is transcriptionally repressed by the metabolic product. We parameterize the gene regulatory model in terms of the promoter characteristic and ribosome binding site (RBS) strengths, both of which are common tuneable knobs in Synthetic Biology. We show that enzymatic saturation imposes bounds on the RBS strength design space. These bounds must be satisfied to prevent metabolite accumulation and guarantee the stability of the network. Simulation results also suggest that the control circuit can effectively upregulate enzyme production to compensate flux perturbations.**

I. Introduction

The main goal of Synthetic Biology is to design cellular systems that carry out customized biological functions. Since the seminal works in [1], [2], the design of gene modules with prescribed functionalities has undergone great progress [3]. One of the most prominent applications of Synthetic Biology is the manipulation of bacterial metabolism for chemical production. Synthetic control of metabolism, however, is still in its infancy and there is a substantial need for genetic control circuits that ensure the robust operation of metabolic pathways under environmental perturbations and cell-to-cell variability [4].

Two landmark implementations of engineered genetic-metabolic circuits are the control of lycopene production [5] and the metabolic oscillator described in [6]. Although it is clear that feedback control is crucial to achieve robust metabolic regulation, only few works have rigorously tackled the general design problem. Notably, the work in [7] demonstrated the use of a synthetic toggle switch [2] as an ON-OFF controller for metabolism, whereas in [8] the authors explored different genetic control architectures for biofuel production.

A common strategy in metabolic engineering is to modify host microbes by expressing heterologous enzymes that convert metabolic intermediates into a chemical of interest [4]. The consumption of intermediates diverts the flux allocated to the native processes of the host (Fig. 1A), potentially affecting its viability.

In this paper we address a synthetic gene circuit aimed at compensating the loss in native flux due to perturbations consuming the intermediates. We focus on an unbranched metabolic pathway under transcriptional repression from the product. We have previously studied the dynamics of multi-promoter circuits in the absence of perturbations, e.g. with a hybrid model and feedback-regulated consumption of the product in [9], and with a continuous model and constant product consumption in [10]. Here we build on the analysis in [10], and investigate an operon control circuit (whereby all the metabolic genes are under the control of a single promoter) under a nonlinear product consumption rate. To ensure the survival of the host cell, the circuit must be able to sustain a metabolic flux that feeds the product into the downstream native processes. Our goal is therefore to identify the constraints in the genetic parameter space that guarantee the existence and stability of a metabolic flux.

We consider a nonlinear ODE model for the feedback system that comprises kinetic equations for the metabolic species and product-dependent enzyme expression (§II). We parameterize the genetic model in terms of the promoter characteristic and the ribosome binding site (RBS) strengths, which are typically used as tuneable knobs in Synthetic Biology applications. We find two bounds for the RBS strengths that guarantee the existence of a steady state, and consequently prevent metabolite accumulation (§III). These bounds appear due to the enzymatic saturation and are sufficient for local stability of the steady state (§IV). We conclude with simulations that illustrate the ability of the control circuit to upregulate enzyme expression and compensate the flux loss due to a branch consuming an intermediate (§V).

II. Unbranched metabolic network under genetic feedback regulation

We consider an unbranched metabolic pathway as in Fig. 1B, where s_0 denotes the concentration of substrate, s_1 is an intermediate metabolite, and s_2 is the metabolic product. The metabolic reactions occur at a rate v_i (each one catalyzed by an enzyme with concentration e_i), and d denotes the product utilization rate. The metabolic genes are encoded in a single operon controlled by a product-responsive transcription factor (TF) that represses enzyme expression (c.f. the multi-promoter system considered in [10]). This kind of transcriptional feedback is common, for example, in bacterial nutrient uptake and amino acid metabolism [11], [12].

A. Metabolic pathway

The network in Fig. 1B exchanges mass with the environment and/or other networks in the cell. The model accounts for this interaction via the input substrate s_0 and the product consumption rate d. Because we are interested in biologically meaningful phenotypes, we assume that s_0 is constant to ensure that the network can reach a nonzero

[†]Centre for Synthetic Biology and Innovation, Department of Bioengineering, Imperial College London, UK; {d.oyarzun,g.stan}@imperial.ac.uk.

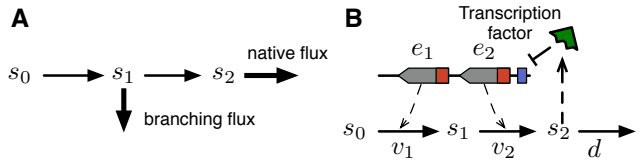

Fig. 1. (A) Engineered metabolic branches divert the flux needed for the host native processes to the synthesis of foreign compounds. (B) Transcriptional repression of an unbranched metabolic pathway by a synthetic operon controlled by a product-responsive transcription factor.

steady state. Note that if the substrate decays, the network eventually reaches a zero equilibrium, whereby the substrate, intermediate metabolites, and product are fully depleted. The constant substrate assumption is also suitable for scenarios where s_0 is an extracellular substrate pool shared by a low density cell population (so that the effects of cell-to-cell competition are negligible).

In a pathway with n reactions and n metabolites, the rate of change of metabolite concentrations can be described by

$$\dot{s}_i = v_i(s_{i-1}, e_i) - v_{i+1}(s_i, e_{i+1}), \tag{1}$$

for $i = 1, 2, \ldots, n$ and $v_{n+1} = d(s_n)$. This model arises from the mass balance between the reactions that produce and consume s_i, and the enzyme kinetics are comprised in the reaction rates $v_i(s_{i-1}, e_i)$. The product consumption rate is typically modeled as a nondecreasing and saturable function, e.g. a Michaelis-Menten type [12] rate of the form

$$d(s_n) = \frac{d_{\max} s_n}{K_{\mathrm{d}} + s_n}, \tag{2}$$

where $d_{\max}$ is the maximal consumption rate and K_{d} is product concentration needed for half-maximal consumption. To keep the analysis as general as possible, we will not presuppose a specific form for the enzyme kinetics. Instead we will generically assume that the metabolic reaction rates are linear in the enzyme concentrations [13]:

$$v_i(s_{i-1}, e_i) = g_i(s_{i-1}) e_i, \tag{3}$$

where g_i is the enzyme turnover rate (i.e. the reaction rate per unit of enzyme concentration). We will also assume that the enzyme turnover rates are nondecreasing and saturable functions of the metabolite concentrations, so that

$$g_i'(s_{i-1}) > 0, \qquad \lim_{s_{i-1} \to \infty} g_i(s_{i-1}) = \hat{g}_i, \tag{4}$$

where $\hat{g}_i$ is the maximal enzyme turnover rate. Assumptions (3)–(4) account for a broad class of irreversible enzyme kinetics [13], e.g. a turnover rate of the form $g_i(s_{i-1}) = k_{\mathrm{cat}\,i} s_{i-1}^q / \left(K_{\mathrm{M}\,i} + s_{i-1}^q\right)$ (where $k_{\mathrm{cat}\,i} = \hat{g}_i$ and $K_{\mathrm{M}\,i}$ is the substrate concentration needed for half saturation) can describe both irreversible Michaelis-Menten (for $q = 1$) and Hill-type (for $q > 1$) kinetics.

B. Transcriptional circuit

In an operon architecture all the enzymes are under the control of a single promoter (for the multi-promoter case see [10]), and thus we model the rate of change of the enzyme concentrations as

$$\dot{e}_i = \underbrace{b_i}_{\substack{\sim\text{RBS} \\ \text{strength}}} \underbrace{\left(\kappa^0 + \kappa^1 \sigma(s_n)\right)}_{\substack{\text{promoter} \\ \text{characteristic}}} - \gamma_i e_i, \tag{5}$$

for $i = 1, 2, \ldots, n$. The equations in (5) come from the balance between protein synthesis degradation (modeled as a linear process with kinetic constant $\gamma_i > 0$). We parameterize enzyme expression in terms of the promoter characteristic and RBS strengths, both of which are common design elements in synthetic gene circuits (see Fig. 2A).

a) Promoter characteristic: It describes the feedback action of product-responsive TFs that repress gene transcription. Promoters are typically described in terms of their *tightness* (κ^0) and *dynamic range* (κ^1), see Fig. 2B. The tightness refers to the level of baseline transcription (i.e. under full repression by the product), whereas the dynamic range is the gap between the ON and OFF transcription levels. We model the regulatory effect of the TF as a Hill function $\sigma(s_n) = \theta^h / \left(\theta^h + s_n^h\right)$ with Hill coefficient $h > 0$ and repression threshold $\theta > 0$. The function σ is a lumped description of the regulatory effect. It does not describe the specific interaction between the product and the TFs, but instead represents the net effect of the product on the transcription rates.

b) RBS strengths: Ribosome binding sites (RBS) are mRNA sequences that are bound by the ribosomes to initiate translation [4]. We model the effect of the RBS strengths as a gain that scales the total expression rate by a factor b_i.

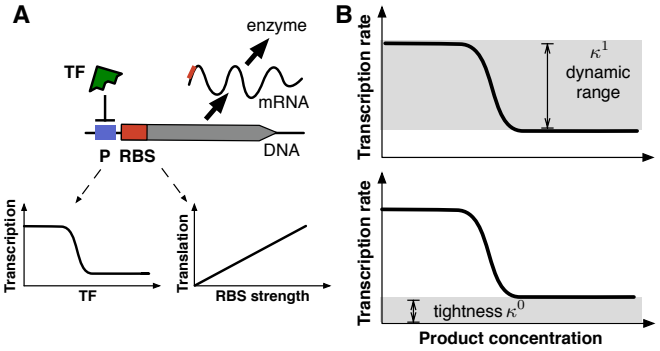

Fig. 2. (A) The promoter characteristic and RBS strengths modulate gene transcription and translation rates, respectively. (B) Typical characteristic of a repressible promoter.

A common strategy in Synthetic Biology is to control protein degradation by adding a degradation tag to the gene sequence [14], and thus we assume that all enzymes are tagged and degraded at the same rate, i.e. $\gamma_i = \gamma$. Altogether, the model for the metabolic network under one-to-all negative regulation reads:

$$\begin{aligned} \dot{s}_i &= g_i(s_{i-1}) e_i - g_{i+1}(s_i) e_{i+1}, \ i = 1, 2, \ldots, n-1, \\ \dot{s}_n &= g_n(s_{n-1}) e_n - d(s_n), \\ \dot{e}_i &= b_i \left(\kappa^0 + \kappa^1 \frac{\theta^h}{\theta^h + s_n^h}\right) - \gamma e_i, \ i = 1, 2, \ldots, n, \end{aligned} \tag{6}$$

with a constant substrate s_0. In the rest of the paper we focus on the properties of the network as a function of the promoter characteristic and RBS strengths.

III. Design constraints caused by enzyme saturation

The operon circuit must be able to sustain a constant metabolic flux that feeds the product into the downstream native processes of the host. In this section we show how this essential requirement translates into constraints on the RBS strength design space.

We will denote the steady state metabolite concentrations, enzyme concentrations, and reaction rates as $\bar{s}_i$, $\bar{e}_i$ and $\bar{v}_i$, respectively, whereas the metabolic flux is $d(\bar{s}_n)$.

A. Existence of the metabolic flux

The regulatory function satisfies $\sigma(s_n) \in (0,1]$ for any product concentration, and therefore from the genetic model (5) we observe that the steady state enzyme concentrations are bounded as $\bar{e}_i \in \left(E_i^{\text{off}}, E_i^{\text{on}}\right]$ with

$$E_i^{\text{off}} = b_i \kappa^0/\gamma, \qquad E_i^{\text{on}} = b_i\left(\kappa^0+\kappa^1\right)/\gamma. \tag{7}$$

The enzyme equilibria can be obtained directly by setting $\dot{e}_i = 0$ in (5)

$$\begin{aligned}\bar{e}_i &= E_i^{\text{off}} + \left(E_i^{\text{on}} - E_i^{\text{off}}\right)\sigma(\bar{s}_n),\\ &= \frac{b_i}{\gamma}\left(\kappa^0+\kappa^1\sigma(\bar{s}_n)\right),\end{aligned} \tag{8}$$

whereas the steady state rates are $\bar{v}_i = g_i(\bar{s}_{i-1})\bar{e}_i$. Because the production utilization $d(s_n)$ saturates at $d_{\max}$, we have the following condition for the existence of a flux.

Proposition 1 (Existence of the flux): The network has a unique metabolic flux $d(\bar{s}_n)$ if and only if the RBS strength of the first enzyme satisfies the bound

$$b_1 < \frac{d_{\max}\gamma}{g_1(s_0)\kappa^0}. \tag{9}$$

Proof: At steady state the first reaction rate must match the consumption rate, so that $\bar{v}_1 = d(\bar{s}_n)$ and the steady state product concentration satisfies

$$d(\bar{s}_n) = g_1(s_0)\bar{e}_1. \tag{10}$$

Combining (8) and (10) we can obtain the product concentration as the solution of

$$\frac{d(\bar{s}_n)}{g_1(s_0)} = \frac{b_1}{\gamma}\left(\kappa^0+\kappa^1\sigma(\bar{s}_n)\right), \tag{11}$$

which can be computed as the intersection of the two curves shown in Fig. 3A. Because of the bound on the utilization rate, equation (11) may not have a solution (see Fig. 3B). From these plots we find that the flux $d(\bar{s}_n)$ exists only when

$$\frac{d_{\max}}{g_1(s_0)} > b_1\frac{\kappa^0}{\gamma}, \tag{12}$$

which is equivalent to the upper bound in (9). Note that since both sides of (11) are monotonic in $\bar{s}_n$, the flux is unique. ■

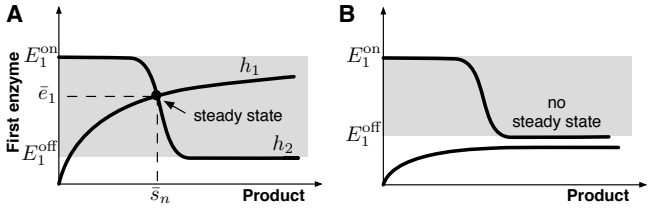

Fig. 3. Existence of the metabolic flux. (A) The solution of (11) can be seen as the intersection of two curves, $h_1(x) = d(x)/g_1(s_0)$ and $h_2(x) = b_1\left(\kappa^0+\kappa^1\sigma(x)\right)/\gamma$. (B) If condition (9) is not met, the curves do not intersect and the flux does not exist.

B. Equilibria of the intermediate metabolites

In operon control all the enzymes are controlled by the product, and therefore the solution of the algebraic equation in (11) also determines the steady state levels of the remaining enzymes ($\bar{e}_i$, $i \geq 2$, see (8)). We must therefore guarantee that the resulting concentrations $\bar{e}_i$ in (8) can effectively sustain their reactions at a rate $d(\bar{s}_n)$.

By setting $\bar{v}_i = d(\bar{s}_n)$ for $i \neq 1$, we can solve for the intermediates from

$$g_i(\bar{s}_{i-1}) = \frac{d(\bar{s}_n)}{\bar{e}_i}. \tag{13}$$

Because the enzyme turnover rates saturate at $\hat{g}_i$, equation (13) has a finite solution only if $d(\bar{s}_n)/\bar{e}_i < \hat{g}_i$, or equivalently

$$\bar{e}_i > \frac{d(\bar{s}_n)}{\hat{g}_i}. \tag{14}$$

A convenient way of analyzing the validity of condition (14) is by defining steady state enzyme levels normalized to their basal and maximal values. We define the normalized enzyme levels $R_i \in (0,1]$ as

$$R_i = \frac{\bar{e}_i - E_i^{\text{off}}}{E_i^{\text{on}} - E_i^{\text{off}}}. \tag{15}$$

With these definitions we can recast condition in (14) as

$$R_i > \hat{R}_i, \tag{16}$$

with

$$\begin{aligned}\hat{R}_i &= \frac{d(\bar{s}_n)/\hat{g}_i - E_i^{\text{off}}}{E_i^{\text{on}} - E_i^{\text{off}}},\\ &= \frac{\gamma}{\kappa^1\hat{g}_i b_i}d(\bar{s}_n) - \frac{\kappa^0}{\kappa^1}.\end{aligned} \tag{17}$$

Condition (16) is a compact description of the design constrains imposed by the saturable nature of enzyme kinetics. We next use it to derive conditions for the existence of the intermediates.

Proposition 2 (Existence of the intermediates): The steady state intermediate concentrations exist if and only if the RBS strengths satisfy

$$\frac{b_i}{b_1} > \frac{g_1(s_0)}{\hat{g}_i}, \text{ for all } i. \tag{18}$$

Proof: The steady state concentration of the first enzyme is $\bar{e}_1 = d(\bar{s}_n)/g_1(s_0)$, and therefore we can write the first expression level R_1 in terms of the flux $d(\bar{s}_n)$

$$R_1 = \frac{d(\bar{s}_n)/g_1(s_0) - E_1^{\text{off}}}{E_1^{\text{on}} - E_1^{\text{off}}}, \\ = \frac{\gamma}{\kappa^1 g_1(s_0) b_1} d(\bar{s}_n) - \frac{\kappa^0}{\kappa^1}. \tag{19}$$

We can readily check that

$$R_1 - \hat{R}_i = \frac{\gamma}{\kappa^1}\left(\frac{1}{b_1 g_1(s_0)} - \frac{1}{b_i \hat{g}_i}\right) d(\bar{s}_n), \tag{20}$$

and therefore the condition in (18) implies $R_1 > \hat{R}_i$. From (8) we note that $R_i = \sigma(\bar{s}_n)$ and therefore all enzymes have the same relative expression levels. In particular, it holds that $R_i = R_1$ for all i, and therefore the RBS bound in (18) also implies that the critical condition (16) is met. ■

Taken together, the conditions in (9) and (18) limit the design space of the RBS strength in terms of the tightness of the promoter (κ^0), the substrate availability (s_0), the saturation of the enzyme kinetics ($\hat{g}_i$) and the maximal product utilization ($d_{\max}$). These conditions therefore depend on a combination of genetic and metabolic parameters, which reflects how the design constraints appear due to the interplay between the enzyme expression and metabolic dynamics.

If the bound for the first enzyme in (9) is not met, the substrate will be consumed at a higher rate than the maximum product utilization, and therefore the design will lead to an infinite accumulation of the product. Analogously, violation of at least one of the bounds in (18) will lead to an infinite accumulation of an intermediate, see Fig. 4A.

In Figs. 4B–C we illustrate the effect of promoter tightness and substrate availability on the feasible region for the RBS strengths. Tighter promoters relax condition (9) and therefore enlarge the feasible region. In the limit case of a perfect "leakless" promoter (i.e. $\kappa^0 = 0$), condition (9) does not limit the RBS strength of the first enzyme. Conversely, an abundant substrate tightens the feasible region via two parallel phenomena: firstly, by condition (9) it limits the RBS strength of the first enzyme to avoid saturation of the product utilization; secondly, by condition (18), more substrate requires a stronger expression of the downstream enzymes to avoid their saturation. These two effects demonstrate how the saturation of enzymes and flux constrains the design space in substrate-rich scenarios.

IV. Stability of the operon control circuit

To examine the local stability of the control circuit, we write the vector of metabolite and enzyme concentrations as s and e, respectively, so that the model can be written as

$$\begin{bmatrix}\dot{s}\\ \dot{e}\end{bmatrix} = \begin{bmatrix} f^s(s,e) \\ f^e(s_n,e)\end{bmatrix}, \tag{21}$$

where the vector fields f^s and f^e can be directly obtained from (6). Our analysis relies on the examination of the structure of the Jacobian matrix of (6), an approach that proved successful in earlier works (e.g. [15] for the case

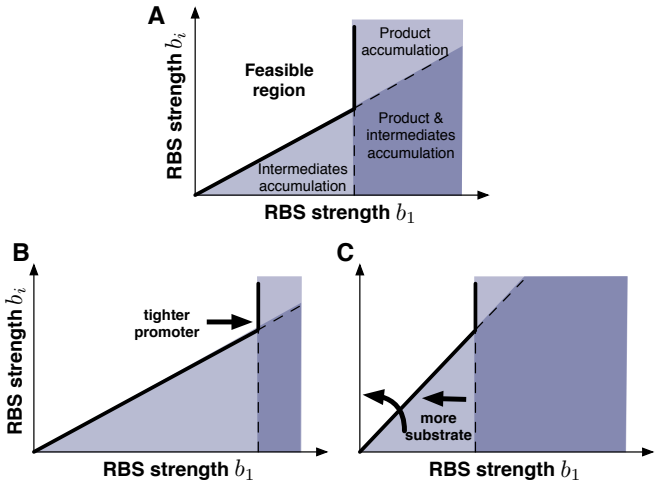

Fig. 4. Design constraints for the RBS strengths. (A) The feasible region prevents the accumulation of intermediates and product; the region is limited by conditions (9) and (18). (B) Tighter promoters enlarge the feasible region, whereas (C) leakier promoters or more substrate tighten the constraints.

of metabolic pathways under product inhibition and linear kinetics). The elements of the Jacobian matrix are

$$\frac{\partial f_i^s}{\partial s_j} = \begin{cases} a_i & j = i-1, \\ -a_{i+1} & j = i, \\ 0 & \text{otherwise}, \end{cases} \tag{22}$$

$$\frac{\partial f_i^e}{\partial s_j} = \begin{cases} \kappa_i^1 \sigma'(\bar{s}_n) & j = n, \\ 0 & \text{otherwise}, \end{cases} \tag{23}$$

$$\frac{\partial f_i^s}{\partial e_j} = \begin{cases} g_i(\bar{s}_{i-1}) & j = i, \\ -g_{i+1}(\bar{s}_i) & j = i+1, \\ 0 & \text{otherwise}, \end{cases} \tag{24}$$

$$\frac{\partial f_i^e}{\partial e_j} = -\gamma, \text{ for all } j. \tag{25}$$

The coefficients a_i are defined as

$$a_i = g_i' \bar{e}_i, \; i = 2, 3, \ldots n, \tag{26}$$

$$a_{n+1} = d', \tag{27}$$

where $g_i' = \partial g_i(s_{i-1})/\partial s_{i-1}|_{\bar{s}_{i-1}}$ and $d' = \partial d(s_n)/\partial s_n|_{\bar{s}_n}$. Note that because g_i and d are nondecreasing it follows that $a_i \geq 0$. We also note that the steady state terms $g_i(\bar{s}_{i-1})$ can be written in terms of the ratio between two enzyme levels as $g_i(\bar{s}_{i-1}) = g_1(s_0)\bar{e}_1/\bar{e}_i$, which using (8) simplifies to $g_i(\bar{s}_{i-1}) = g_1(s_0) b_1/b_i$. We can therefore write the Jacobian as a block matrix $J = \begin{bmatrix} J_{11} & J_{12} \\ J_{21} & J_{22}\end{bmatrix}$, where the four blocks are $n \times n$ matrices

$$J_{11} = \begin{bmatrix} -a_2 & 0 & 0 & \cdots & 0 \\ a_2 & -a_3 & 0 & \cdots & 0 \\ 0 & a_3 & \ddots & \ddots & \vdots \\ \vdots & \ddots & \ddots & -a_n & \vdots \\ 0 & \cdots & \cdots & a_n & -d' \end{bmatrix}, \tag{28}$$

$$J_{12} = g_1(s_0)b_1 \begin{bmatrix} b_1^{-1} & -b_2^{-1} & 0 & \cdots & 0 \\ 0 & b_2^{-1} & -b_3^{-1} & \cdots & 0 \\ 0 & 0 & b_3^{-1} & \ddots & \vdots \\ \vdots & \ddots & \ddots & \ddots & -b_n^{-1} \\ 0 & \cdots & \cdots & \cdots & b_n^{-1} \end{bmatrix}, \quad (29)$$

$$J_{21} = \kappa^1 \sigma' \begin{bmatrix} 0 & \cdots & 0 & b_1 \\ \vdots & \ddots & \ddots & b_2 \\ \vdots & \ddots & \ddots & \vdots \\ 0 & \cdots & 0 & b_n \end{bmatrix}, \qquad J_{22} = -\gamma I, \quad (30)$$

and $\sigma' = \partial\sigma(s_n)/\partial s_n|_{\bar{s}_n}$. With these definitions, we have the following stability result.

Proposition 3 (Local stability): Under the conditions of Propositions 1 and 2, the network has a locally stable steady state. Moreover, its Jacobian has:

- $n-1$ stable eigenvalues at $\lambda = -\gamma$,
- $n-1$ stable eigenvalues at $\lambda = -a_i$, $i = 2, 3, \ldots, n$,
- and two stable eigenvalues at

$$\lambda = \frac{-(d'+\gamma) \pm \sqrt{(d'-\gamma)^2 + 4\kappa_1^1 \sigma' g_1(s_0)}}{2}. \quad (31)$$

Proof: This is an extension of Propositions 2 and 3 in [10] to the case of a saturable consumption rate $d(\bar{s}_n)$. ■

Proposition 3 provides useful analytic expressions for the modes of the feedback system and has two main consequences. First, the repeated eigenvalues at $\lambda = -\gamma$ are independent of the circuit design parameters, and hence they correspond to *fixed modes* of the control circuit. Although they can be adjusted by changing the degradation rate (e.g. by using various degradation tags), they cannot be suppressed by fine tuning the regulatory parameters and they translate into $(n-1)$ modes of the form $e^{-t/\gamma}$, $te^{-t/\gamma}$, ..., $t^{n-2}e^{-t/\gamma}$. Enzyme degradation rates are inversely proportional to their half-lives, which are in turn much longer than metabolic time scales (half-lives are in the order of minutes to hours, whereas metabolic time scales are typically milliseconds to seconds [13]). Therefore, depending on the initial conditions the network can potentially display very slow transients, and this appears to be aggravated in long pathways.

Second, we observe that as the steady state product grows, both d' and σ' tend to vanish, and therefore one of the eigenvalues in (31) approaches the imaginary axis. This implies that, although in principle the promoter dynamic range κ^1 and RBS strength b_1 can be designed to maximize the flux (i.e. by shifting the steady state $\bar{s}_n$ towards the right in Fig. 3A we get a higher flux $d(\bar{s}_n)$), this can only be done at the expense of a dramatic reduction in the response speed.

V. Flux compensation by enzyme upregulation

A common strategy in metabolic engineering is to modify bacteria by expressing heterologous enzymes that convert natural metabolic intermediates into a compound of interest [4]. Since the target compound is synthesized by "branching out" a specific intermediate from a natural pathway, part of the metabolic flux needed to sustain the host native processes is redirected to the production of the foreign chemical. In this section we show simulation results suggesting that a synthetic operon circuit can dramatically dampen the effect of perturbations on the native flux.

To account for a branch consuming an intermediate s_j at a rate $d_{\rm ext}$, we modify the model in (6) by including $d_{\rm ext}$ as a consumption rate in the ODE for s_j

$$\dot{s}_j = g_i(s_{i-1})e_i - g_{i+1}(s_i)e_{i+1} - d_{\rm ext}. \quad (32)$$

We can show that the branch introduces an additional lower bound for the RBS strength of the first enzyme. This bound adds on to the ones in Propositions 1 and 2, and has the form $b_1 > \bar{d}_{\rm ext}\gamma / \left(g_1(s_0)\left(\kappa^0 + \kappa^1\right)\right)$, where $\bar{d}_{\rm ext}$ is the steady state value of $d_{\rm ext}$ (we omit the details due to length constraints).

To illustrate the dynamic response of the feedback circuit, we simulate the network in Fig. 1B under a flux perturbation that consumes the intermediate s_1. We consider a pathway with two metabolites and two enzymes with Michaelis-Menten kinetics with $k_{{\rm cat}\,i} = 32{\rm s}^{-1}$ and $K_{{\rm M}\,i} = 4.7\mu{\rm M}$. These are representative values for PRA isomerase (extracted from the BRENDA database, EC number 5.3.1.24), a transcriptionally regulated enzyme involved in the tryptophan pathway of *E. coli*. We use a substrate concentration $s_0 = K_{{\rm M}\,1}$ (so that $g_1(s_0)$ is at half-saturation) and we use product consumption parameters $d_{\max} = 0.416\mu{\rm Ms}^{-1}$ and $K_{\rm d} = 0.2\mu{\rm M}$, both taken from an experimentally validated model for the tryptophan pathway [12]. The enzyme degradation rate is $2 \times 10^{-4}{\rm s}^{-1}$ (half-life $\sim$1h), whereas the promoter parameters are $\theta = K_{\rm d}$, $h = 2$. We consider a promoter of up to 100-fold repression (i.e. we take $(\kappa^0+\kappa^1)/\kappa^0 = 100$), and choose κ^1 so that the maximal steady state enzyme levels are $E_1^{\rm on} = 0.25\mu{\rm M}$ and $E_2^{\rm on} = 1\mu{\rm M}$ for RBS strengths $b_i = \{1, 4\}$. These RBS strengths comply with the feasible region of Fig. 4 and the $E_i^{\rm on}$ values are within the physiological range of *E. coli* [16].

Before the perturbation (induced at 500min), the network is in steady state with a flux $\sim$19.5$\mu{\rm M}/{\rm min}$. We model the branch as an S-shaped rate that reaches 75% of the pre-stimulus flux in $\sim$1hr. The simulations in Fig. 5 show how the synthetic operon circuit upregulates enzyme expression by $\sim$68% in response to the activation of the branch. In terms of both flux and product concentration, we observe a dramatic improvement compared to open loop case (i.e. with unregulated constant enzyme concentrations chosen to match the pre-stimulus flux): the operon circuit compensates the loss in native flux from 75% (open loop) to $\sim$7.5%, whereas the drop in steady state product concentration is brought down from $\sim$93% (open loop) to $\sim$27%.

VI. Discussion & outlook

We have presented a detailed analysis of a synthetic gene circuit aimed at controlling an unbranched metabolic pathway. The goal of this control system is to dampen flux perturbations that divert the native flux to the production of foreign molecules. The control strategy relies on encoding the metabolic genes in a single operon repressed by a

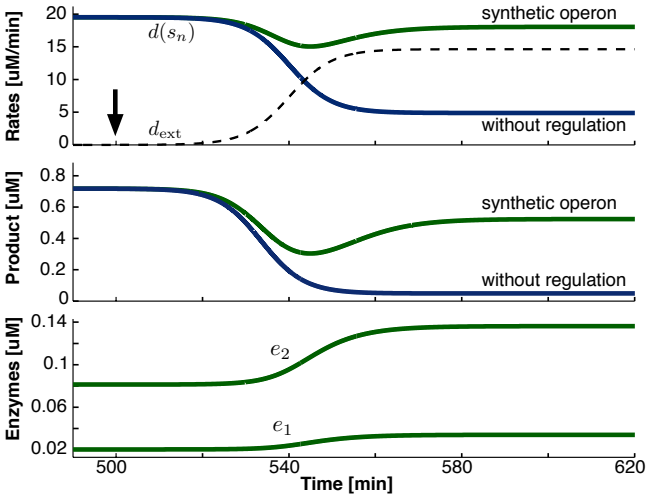

Fig. 5. Dynamic response of the operon control circuit to a flux perturbation and comparison with the open loop case (i.e. with constant enzyme concentrations). The dashed line is the rate at which the intermediate is drained from the pathway (d_{ext}), starting at $t = 500$min (arrow).

product-responsive TF. This architecture allows for enzyme upregulation in response to a drop in the metabolic product concentration, thereby compensating the loss in flux.

Genetic control of metabolism has been extensively studied in the case of natural systems. These studies typically focus on understanding how observed phenotypes emerge from the genetic-metabolic crosstalk [9], [17], and a number of detailed mechanistic models for operon regulation have been developed [11], [12]. In Synthetic Biology, however, the goal is to design regulatory circuits for controlling metabolism in a customized fashion. Model-based design therefore requires mathematical descriptions that are explicitly parameterized in term of common biological knobs used in Synthetic Biology. Consequently, our model is deliberately not mechanistic, and instead describes the genetic feedback in terms of tuneable parameters such as the promoter's dynamic range, RBS strengths and protein half-lives.

Our analysis has revealed a number of constraints in RBS strength design space. These need to be satisfied to prevent metabolite accumulation and guarantee the stability of the network. The bounds depend on a combination of transcriptional and kinetic parameters, thereby highlighting how the design constraints appear due to the interplay between the genetic and metabolic subsystems. Simulations of the feedback system with realistic parameter values show promising results, suggesting that the proposed control strategy can effectively compensate the effect of flux perturbations on the host native processes.

We remark that the derived design constraints are only baselines for the functioning of the circuit. In most applications the design must also account for objectives such as maximization of yield or minimization of transcriptional effort. These multi-objective design problems require the use of optimization methods to search for optimal combinations of feedback parameters within the feasibility sets derived here. In addition, in this work we have considered an unbranched pathway in isolation from the other cellular pathways. In practical applications, the cross-talk between pathways may have a detrimental impact on the performance of the control circuit, and therefore we are carrying out further investigations to account for branched metabolic pathways.

The wetlab implementation of genetic-metabolic circuits can be costly and time consuming. Our work provides new insights into which factors need to be addressed at a design stage, potentially facilitating the implementation in future Synthetic Biology applications.

VII. Acknowledgements

We thank Dr John Heap for fruitful discussions and all the members of the Stan group at Imperial College London.

References

[1] M. B. Elowitz and S. Leibler, "A synthetic oscillatory network of transcriptional regulators," *Nature*, vol. 403, no. 6767, pp. 335–338, Jan. 2000.

[2] T. S. Gardner, C. R. Cantor, and J. J. Collins, "Construction of a genetic toggle switch in Escherichia coli," *Nature*, vol. 403, no. 6767, pp. 339–342, Jan. 2000.

[3] T. K. Lu, A. S. Khalil, and J. J. Collins, "Next-generation synthetic gene networks." *Nature biotechnology*, vol. 27, no. 12, pp. 1139–50, Dec. 2009.

[4] W. J. Holtz and J. D. Keasling, "Engineering static and dynamic control of synthetic pathways." *Cell*, vol. 140, no. 1, pp. 19–23, Jan. 2010.

[5] W. R. Farmer and J. C. Liao, "Improving lycopene production in Escherichia coli by engineering metabolic control," *Nat Biotech*, vol. 18, no. 5, pp. 533–537, May 2000.

[6] E. Fung, *et al.*, "A synthetic gene-metabolic oscillator," *Nature*, vol. 435, no. 7038, pp. 118–122, May 2005.

[7] N. Anesiadis, W. R. Cluett, and R. Mahadevan, "Dynamic metabolic engineering for increasing bioprocess productivity," *Metabolic Engineering*, vol. 10, no. 5, pp. 255–266, Sept. 2008.

[8] M. J. Dunlop, J. D. Keasling, and A. Mukhopadhyay, "A model for improving microbial biofuel production using a synthetic feedback loop," *Systems and Synthetic Biology*, vol. 4, no. 2, pp. 95–104, 2010.

[9] D. A. Oyarzún, M. Chaves, and M. Hoff-Hoffmeyer-Zlotnik, "Multistability and oscillations in genetic control of metabolism." *Journal of Theoretical Biology*, vol. 295, pp. 139–153, 2012.

[10] D. A. Oyarzún and G.-B. Stan, "Design tradeoffs in a synthetic gene control circuit for metabolic networks," in *Proceedings of the 31st American Control Conference*, Montreal, 2012, pp. 2743–2748.

[11] N. Yildirim and M. C. Mackey, "Feedback regulation in the lactose operon: A mathematical modeling study and comparison with experimental data," *Biophysical Journal*, vol. 84, no. 5, pp. 2841–2851, May 2003.

[12] M. Santillán and M. C. Mackey, "Dynamic regulation of the tryptophan operon: A modeling study and comparison with experimental data," *Proceedings of the National Academy of Sciences of the United States of America*, vol. 98, no. 4, pp. 1364–1369, Feb. 2001.

[13] A. Cornish-Bowden, *Fundamentals of Enzyme Kinetics*, 3rd ed. Portland Press, 2004.

[14] K. E. McGinness, T. A. Baker, and R. T. Sauer, "Engineering controllable protein degradation." *Molecular cell*, vol. 22, no. 5, pp. 701–7, June 2006.

[15] J. Tyson and H. Othmer, "The dynamics of feedback control circuits in biochemical pathways," *Progress in Theoretical Biology*, vol. 5, pp. 1–62, 1978.

[16] E. Levine and T. Hwa, "Stochastic fluctuations in metabolic pathways." *Proceedings of the National Academy of Sciences of the United States of America*, vol. 104, no. 22, pp. 9224–9, May 2007.

[17] V. Baldazzi, *et al.*, "Importance of metabolic coupling for the dynamics of gene expression following a diauxic shift in Escherichia coli." *Journal of theoretical biology*, vol. 295, pp. 100–115, 2012.